JOURNAL OF VIROLOGY, Dec. 1997, p. 9214–9222 Vol. 71, No. 12
0022-538X/97/$04.00+0

Canine Parvovirus Host Range Is Determined by the Specific Conformation of an Additional Region of the Capsid

JOHN S. L. PARKER AND COLIN R. PARRISH*

James A. Baker Institute for Animal Health, College of Veterinary Medicine, Cornell University, Ithaca, New York 14853

Received 16 December 1996/Accepted 3 September 1997

We analyzed a region of the capsid of canine parvovirus (CPV) which determines the ability of the virus to infect canine cells. This region is distinct from those previously shown to determine the canine host range differences between CPV and feline panleukopenia virus. It lies on a ridge of the threefold spike of the capsid and is comprised of five interacting loops from three capsid protein monomers. We analyzed 12 mutants of CPV which contained amino acid changes in two adjacent loops exposed on the surface of this region. Nine mutants infected and grew in feline cells but were restricted in replication in one or the other of two canine cell lines tested. Three other mutants whose genomes contain mutations which affect one probable interchain bond were nonviable and could not be propagated in either canine or feline cells, although the VP1 and VP2 proteins from those mutants produced empty capsids when expressed from a plasmid vector. Although wild-type and mutant capsids bound to canine and feline cells in similar amounts, infection or viral DNA replication was greatly reduced after inoculation of canine cells with most of the mutants. The viral genomes of two host range-restricted mutants and two nonviable mutants replicated to wild-type levels in both feline and canine cells upon transfection with plasmid clones. The capsids of wild-type CPV and two mutants were similar in susceptibility to heat inactivation, but one of those mutants and one other were more stable against urea denaturation. Most mutations in this structural region altered the ability of monoclonal antibodies to recognize epitopes within a major neutralizing antigenic site, and that site could be subdivided into a number of distinct epitopes. These results argue that a specific structure of this region is required for CPV to retain its canine host range.

Host range is a fundamental and stable property of animal viruses which determines the animals or cells that are susceptible to infection. Capsid proteins determine the host range of many parvoviruses, including canine parvovirus (CPV), feline panleukopenia virus (FPV), mink enteritis virus (9, 22, 34, 44, 45), minute virus of mice (2, 3, 18, 19), Aleutian mink disease virus (8), and porcine parvovirus (6, 49). CPV, a newly emerging member of the feline parvovirus subgroup of the autonomous parvoviruses, has an extended host range compared to that of the closely related FPV (32, 33).

CPV is a small, nonenveloped virus containing a single-stranded DNA genome of negative polarity. The CPV capsid is a 26-nm-diameter icosahedron made up of 60 copies of a combination of capsid proteins VP1 and VP2, with between 6 and 10 copies of VP1 per particle (13, 30). The capsid protein structure was determined to near-atomic resolution by X-ray crystallography. The structure of the capsid monomer from residue 37 to the C terminus of VP2 was visible (47). The core of each capsid monomer is comprised of an eight-stranded antiparallel β-barrel which has four extensive loops connecting the β-strands. These loops form most of the capsid outer surface. The surface features of the capsid include a hollow cylinder at the fivefold axis of symmetry which is surrounded by a circular depression (termed the canyon), a prominent protrusion at the threefold axis of symmetry (threefold spike), and a depression (called the dimple) spanning the twofold axis of symmetry.

CPV can replicate in both canine and feline cells in cultures, whereas FPV can replicate in feline but not canine cells (46). The determinants of the in vitro canine host range difference between CPV and FPV have been mapped to residues 93 and 323 of capsid protein VP2 (9). These surface residues lie on the capsid threefold spike. If both residues Lys-93 and Asp-323 in FPV are changed to Asn, the resulting mutant is able to replicate in canine cells in vitro, whereas mutating either Asn-93 or Asn-323 in CPV to Lys or Asp, respectively, results in a loss of the in vitro canine host range (9).

A mutant of CPV (CPV 102/10) derived by 102 passages in primary dog kidney cells and 10 passages in NLFK cells is unable to replicate in canine A72 cells and differs antigenically from its parental strain (37). The region involved in the antigenic variation and host range of CPV 102/10 maps between the *Bgl*II and *Pvu*II sites (map units 64 to 73) in the viral genome. The sequence of this region in CPV102/10 differs by 8 nucleotides from that in CPV-d (a wild-type isolate), leading to 4 amino acid differences in capsid proteins VP1 and VP2. These are VP2 residues Lys-271→Arg, Ala-300→Asp, Thr-301→Ile, and Val-316→Ile. The changes at residues 271 and 316 are also found in CPV-94, a strain of CPV that is able to infect canine A72 cells in cultures (37). Therefore, of the four changed residues, only residues 300 and 301 appear to be associated with the loss of the in vitro canine host range.

Residues 300 and 301 of VP2 are located on loop 3 of the VP2 monomer structure. They are surface-exposed residues and form part of a region on a ridge of the threefold spike of the capsid termed the shoulder. This region is comprised of five polypeptide loops from three different capsid proteins (1, 47). Two dominant neutralizing antigenic sites (sites A and B) map to the threefold spike of the capsid, and residues 300 and 301 of VP2 form part of neutralizing site B (42, 50).

The structure of a CPV mutant containing the Ala-300→Asp mutation has been solved. The aspartic acid substitution at residue 300 leads to the formation of a new salt bridge with Arg-81 on a threefold axis-related VP2 monomer as well

* Corresponding author. Phone: (607) 256-5649. Fax: (607) 256-5608. E-mail: crp3@cornell.edu.

as changes in the structure of loop 3 around the mutation (26). It has been suggested that the formation of a new salt bridge between the two surface loops might lead to increased stability of the virus particle (26).

We hypothesized that the conformation of the shoulder region in the capsid of CPV is critical for infection of canine cells and that salt bridges within this region may be important for both conformation and stability. We analyzed several viruses with changes in the shoulder region of the threefold spike of the capsid and found that the specific capsid conformation in this region is critical for both the ability to infect canine cells and virus viability. The restriction of the canine host range conferred by mutations within the shoulder region of the CPV capsid appears to occur at an early stage of viral infection, before replication but after cell binding. The mutants also demonstrated the presence of a number of distinguishable epitopes within antigenic site B.

MATERIALS AND METHODS

Cells and viruses. NLFK and canine A72 cells were grown in a 1:1 mixture of McCoy's 5A and Leibovitz L15 media with 5% fetal bovine serum (7, 16). The MDCK cell line (clone AA7; type I strain) (29) was obtained from W. W. Young, University of Kentucky, and grown in Dulbecco's modified minimal essential medium (DMEM) with 10% fetal bovine serum.

Mutations were prepared in the infectious plasmid clone (pBI265) derived from CPV-d, a wild-type isolate of CPV type 2 (34, 36). Virus stocks were prepared by electroporation or by Lipofectamine (GIBCO BRL, Bethesda, Md.)-mediated transfection of NLFK cells with plasmids. Virus titrations were performed by an immunostaining plaque method as described previously (37), except that foci of virus-infected cells were detected with rabbit polyclonal antisera against intact CPV capsids. Bound antibody was visualized with horseradish peroxidase (HRPO)-conjugated goat anti-rabbit antiserum and the HRPO substrate 3-amino-9-ethyl-carbazole. Viruses were also titrated by a 50% tissue culture infective dose ($TCID_{50}$) assay on NLFK cells in 96-well trays; the cells were fixed after 2 days and then stained by an immunoperoxidase assay. Infected cells were detected by microscopy, and the $TCID_{50}$ was calculated by the method of Reed and Muench (39).

To prepare intact virus capsids, viruses were grown in NLFK cells in roller bottles for 4 to 6 days. Virus-containing medium was collected, and the cells were discarded. The medium was clarified by centrifugation at 5,200 × *g* for 15 min, 0.1% (vol/vol) Nonidet P-40 was added to the supernatant, and the virus was concentrated by ultrafiltration with a 10^6-Da-cutoff polyvinylidene fluoride membrane filter (Spectrum, Houston, Tex.). The retained material (~30 ml) was turbid; after it was clarified by low-speed centrifugation (3,800 × *g* for 20 min at 4°C), we found that the majority of the virus was present in the pellet (31). The virus-containing pellet was resuspended in 2 ml of 10 mM Tris-HCl (pH 7.4)–100 mM NaCl (Tris-saline), and the virus was centrifuged in a 10 to 30% (vol/vol) glycerol gradient in Tris-saline for 3 h at 82,000 × *g* and 25°C. The empty and full (DNA-containing) capsids were washed and concentrated by Centricon-50 ultrafiltration and then stored at 4°C in Tris-saline or at −20°C in Tris-saline with 50% glycerol.

Mutagenesis, virus recovery, and capsid protein expression. As shown in Fig. 1, the capsid structure in the region around VP2 residue 300 is complex. To examine the role of this region in the functions of CPV, mutant viral genomes were prepared (Fig. 2A). Some mutants contained various combinations of the amino acid changes found in CPV 102/10. Others were initially detected as neutralization escape mutants (42) or were designed to specifically affect predicted interactions between VP2 loops (Fig. 1C and 2A). Site-directed mutations were prepared in an M13 clone containing part of the VP2 gene by use of specific oligonucleotides and the method of Kunkel (25, 43). The region from the *Spe*I site to the *Eco*RV site (CPV genome map units 67 to 79) of the mutated M13 phage was sequenced. That restriction fragment was used to replace the same region of the infectious plasmid clone of CPV-d (34). Mutants were named after the VP2 amino acid substitutions that they contained by use of the single-letter code—i.e., a change of VP2 residue 300 from Ala to Asp is shown as A300D.

Viruses could not be recovered from three plasmids, and the VP1 and VP2 genes of those plasmids were cloned into the expression vector pcDNA1-neo (Invitrogen, San Diego, Calif.) as described previously (43). A72 cells were transfected with the expression plasmids by use of Lipofectamine and then selected with 400 μg of G418 per ml. The cells were lysed by freezing-thawing twice, the capsids were concentrated by precipitation with 4% (wt/vol) polyethylene glycol (molecular weight, 8,000). The buoyant densities of purified empty capsids were compared on isopycnic CsCl gradients (initial density, 1.32 g of CsCl per cm^3) centrifuged at 240,000 × *g* for 24 h at 15°C (43).

Antigenic analysis. Viruses or plasmid-expressed capsids were antigenically typed with a panel of monoclonal antibodies (MAbs) prepared against CPV type 2, CPV type 2b, or FPV capsids (36, 38, 42). Hemagglutination (HA) inhibition (HI) assays were used to determine the reactivity of the MAbs to each virus, as all the MAbs used inhibit HA (42). Several viruses were further tested in an enzyme-linked immunosorbent assay (ELISA) as described previously (42).

Host range analysis. To test for cell infection, wild-type and mutant viruses prepared by plasmid transfection and one or two passages in NLFK cells were titrated by a $TCID_{50}$ assay in NLFK, A72, or MDCK cells as described above.

To examine for viral DNA replication, NLFK and A72 cells were inoculated with each virus at a multiplicity of ~0.1 $TCID_{50}$ per cell and incubated for 72 h. MDCK-AA7 cells were similarly treated but were incubated for 48 h to allow optimal recovery of viral DNA. Cells were lysed into 0.15 M NaCl–10 mM Tris-HCl (pH 7.5)–10 mM EDTA–2% sodium dodecyl sulfate (SDS) with 200 μg of proteinase K per ml and incubated for 1 h at 37°C. The lysate was extracted with phenol-chloroform, and the DNA was precipitated with ethanol. The DNA was electrophoresed in 1% agarose gels containing 1 μg of ethidium bromide per ml, transferred to nylon membranes, and detected by hybridization with a DNA probe comprised of the complete CPV genome labeled with [^{32}P]dCTP.

Viral DNA replication after plasmid transfection. Cells were transfected with plasmids containing the genomes of CPV-d, G299E, K387A, E298A, and T389A. Briefly, NLFK or A72 cells seeded at 10^4 cells/cm^2 in 9-cm^2 wells were synchronized by a combination of isoleucine deprivation for 24 h followed by aphidicolin treatment for 20 h (13, 48). The cells were transfected with 5 μg of DNA by use of 8 μl of Lipofectamine. Total-cell DNA was recovered 72 h after transfection as described above. DNA samples were digested for 3 h with 10 U of *Dpn*I in 50 mM Tris-HCl (pH 8.0)–10 mM $MgCl_2$–210 mM NaCl–1 mM dithiothreitol and then electrophoresed and analyzed as described above.

Capsid binding assays. NLFK cells were infected with 1 PFU of CPV-d, G299E, or K387A per cell. After 24 h, they were labeled with [^{35}S]methionine for 6 h. The cells were lysed into 0.1 M Tris-HCl (pH 8.0)–1% Nonidet P-40, the lysate and the cell medium were combined and clarified by low-speed centrifugation, and the virus was pelleted at 200,000 × *g* for 2 h at 4°C. Capsids were purified on 10 to 40% sucrose gradients, and the full and empty particles were collected separately. Empty viruses diluted in DMEM to give 20,000 cpm of virus per inoculum were bound to 5×10^5 NLFK, A72, or MDCK cells at 4°C for 1 h in duplicate. The cells were washed three times with DMEM at 4°C, lysed into 1 ml of 0.1 N NaOH, and subjected to scintillation counting. Specific activities were estimated from the amount of protein detected by Western blotting of 10,000 cpm of each labeled virus preparation.

Capsid stability. (i) Temperature inactivation. Preliminary studies showed that CPV-d infectivity was sensitive to heating at 75°C. CPV-d, G299E, and K387A were incubated at 75°C for 5, 10, 20, and 40 min. The titers of surviving PFU in each sample were determined in NLFK cells in triplicate.

(ii) Stability against denaturation. Purified capsids in bis–Tris-HCl (50 mM)–NaCl (150 mM) at pH 7.5, 7.0, or 6.0 were incubated with urea at final concentrations of 3.0 to 8.0 M or were left untreated. Capsids were then bound to nitrocellulose membranes in a slot-blot apparatus. The membranes were washed with Tris-saline (pH 7.4) and incubated with rabbit anti-CPV capsid serum (anticapsid serum), rabbit anti–SDS-denatured capsid serum (anti-VP1/VP2 serum), or a mouse serum prepared against a synthetic peptide containing the sequence of VP2 residues 258 to 270 (anti–258-270 serum). Filters were incubated with HRPO-conjugated goat anti-rabbit immunoglobulin G (IgG) or anti-mouse IgG and then with Supersignal chemiluminescence substrate (Pierce Chemical, Indianapolis, Ind.) and exposed to X-ray film.

RESULTS

Studies of the CPV 102/10 mutant indicated that mutations affecting the canine host range were most likely located within or near the shoulder of the threefold spike of the CPV capsid (37, 47). To further define the role of this region in the control of host range, we prepared 12 different full-length plasmid clones with various mutations (Fig. 2A). Nine different mutant viruses were isolated after transfection of NLFK cells, while no viruses were recovered in multiple attempts from the other three plasmids (Fig. 2B). The latter (E298A, K387A/T389A, and T389A) were therefore considered nonviable. Empty capsids prepared from A72 cells transfected with a mammalian expression vector containing the VP1 and VP2 genes of the nonviable mutants had the same buoyant density as CPV-d empty capsids, and they also hemagglutinated erythrocytes (Fig. 3).

Host range. As shown in Fig. 2, the relative abilities of the mutant viruses to infect the cell lines tested revealed three patterns of host range restriction: (i) mutant viruses which were severely restricted (>100-fold) in their ability to infect both canine cell lines tested—mutants G299E, G299D, K387A, and A300D/T301I/V316I; (ii) mutant viruses which were se-

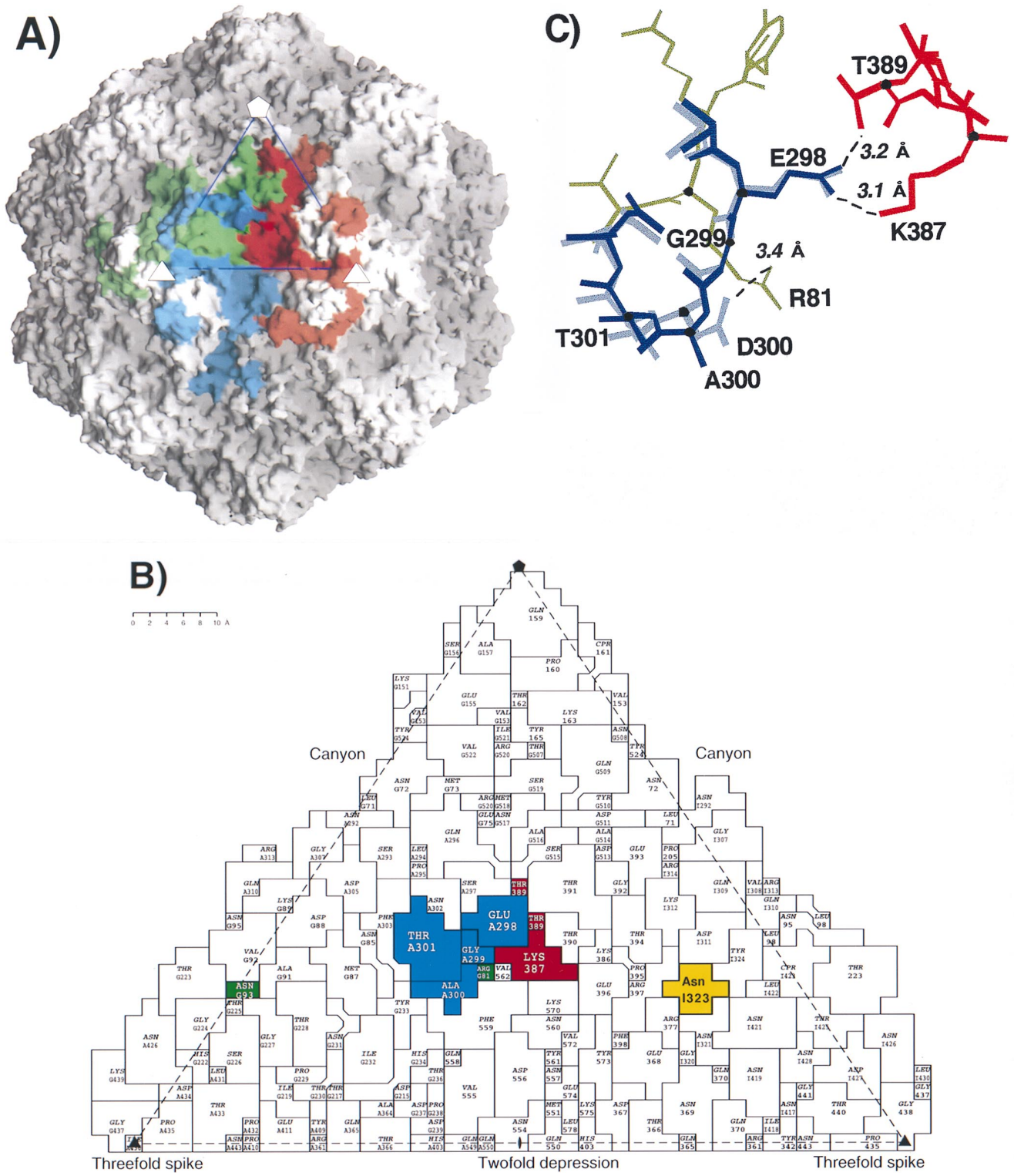

FIG. 1. Structure of the capsid and of the shoulder region. (A) Representation of the molecular surface of the CPV capsid with radial depth cueing, viewed along the icosahedral twofold axis. The large triangle indicates the location of one asymmetric unit of the icosahedral structure. Three of the VP2 molecules which interact in the shoulder region are shown in green, blue, and red. (B) "Road map" showing the surface-exposed portions of amino acids within one asymmetric unit of the CPV capsid (40). The residues mentioned in this study are colored differently according to their locations on various VP2 monomers. VP2 residues 93 and 323, which differ between CPV and FPV, were shown in previous studies to control infection of canine cells (9), while residue Arg-81 interacts with residue Asp-300 in mutant A300D (26). (C) Detailed molecular structure of the surface polypeptide loops of the shoulder region. Hydrogen bonds between residues on different subunits are indicated by broken lines. The three protein subunits are shown in red, blue, and green, and amino acids are numbered as in VP2. The view is in the same orientation as in panels A and B. Differences determined by X-ray crystallography in the structure of mutant A300D are shown in the model with the crosshatched blue line.

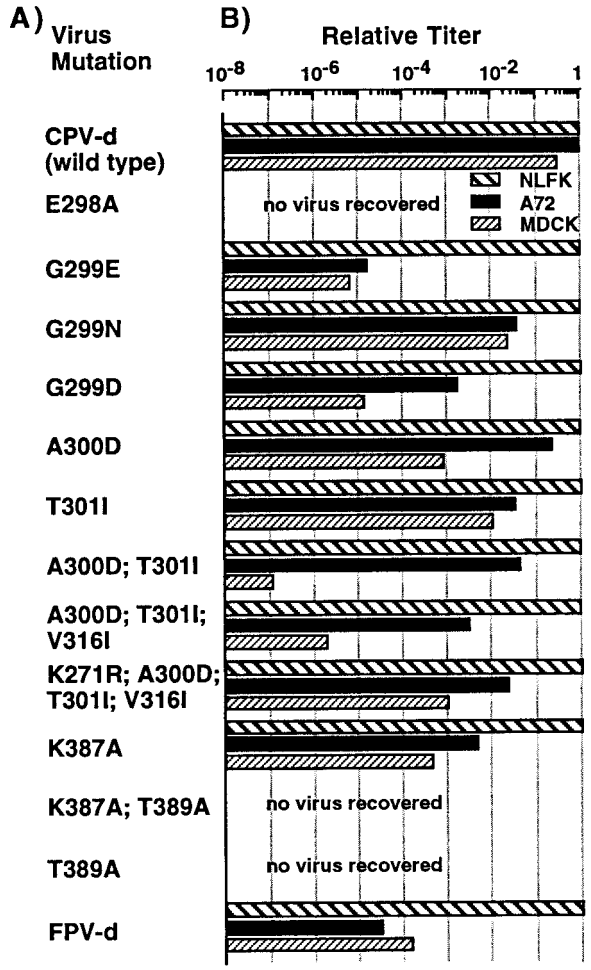

FIG. 2. Mutants prepared in this study. (A) Mutation(s) present in each virus. (B) Comparative titers of viruses in NLFK, A72, and MDCK cells. Virus stocks were titrated in NLFK, A72, and MDCK cells by a $TCID_{50}$ assay. For each virus, titers in A72 and MDCK cells are shown relative to those in NLFK cells. FPV-d, wild-type FPV.

verely restricted in their ability to infect MDCK cells but which infected and replicated in A72 cells—mutants A300D, and A300D/T301I; (iii) mutant viruses which infected both canine cell lines but to a 1- to 2-log_{10}-lower titer than that seen in NLFK cells—G299N and T301I. Mutant G299E was about 10^5-fold less infectious for both A72 and MDCK cells than for NLFK cells and thus was similar to FPV in host range restriction in these canine cells (Fig. 2B).

The host ranges of the mutant viruses were also assayed by comparing viral DNA replication following infection with equivalent NLFK $TCID_{50}$ titers of CPV-d and the mutant viruses, and similar results were observed (Fig. 4). Some mutant viruses—K387A, G299E, and G299D—produced little or no replicative-form (RF) DNA in either canine cell line. A300D replicated to a level equivalent to that of CPV-d in A72 cells but not in MDCK cells, while G299N and T301I replicated in both cell types but to higher and lower levels, respectively, than CPV-d (Fig. 4).

From the data given above, we conclude that MDCK cells were more restrictive than A72 cells for most of the mutant viruses (Fig. 2B and 4) and that the host ranges being examined are dependent on both the mutant virus and the canine cell. It is apparent from the data presented in Fig. 2B and 4 that although mutants G299D and T301I had lower relative $TCID_{50}$ titers in the canine cell lines than in NLFK cells, they appeared to be able to replicate their genomes to levels equivalent to or higher than that reached by CPV-d in the canine cells. We attribute this consistent finding to differences in the nature and sensitivity of the two assays.

Binding to NLFK, A72, and MDCK cells. CPV-d, G299E, and K387A virions were labeled with [^{35}S]methionine and used in cell binding assays. Mutant K387A bound to all cells to a greater extent than CPV-d, which bound more than G299E. Relatively more of all three viruses bound to MDCK cells than to NLFK cells, while less virus bound to A72 cells than to NLFK cells (Fig. 5). Thus, the host range difference between the mutant viruses and CPV-d cannot be explained simply by differences in binding to the surfaces of the different cells.

DNA replication after plasmid transfection. CPV-d, G299E, K387A, E298A, and T389A were transfected as full-length plasmid clones, and all replicated to produce monomer RF (mRF) and dimer RF (dRF) viral DNAs in A72 cells (Fig. 6). Single-stranded viral DNA could not be quantified after transfection with the plasmids, as a *Dpn*I-derived plasmid DNA band ran in the same position in the gel (31).

Antigenic structure. The structure of antigenic site B was altered in 9 of 12 mutant capsids, as demonstrated by the reduced HI titer of MAb 16 (Fig. 7A). Changes at residues 299, 300, and 387 all resulted in changes in the antibody recognition of antigenic site B (Fig. 7A). A change of Gly at residue 299 to Asn, Asp, or Glu caused a loss of reactivity of MAbs 15 and 16, either together or separately. All of the site B-specific MAbs that we tested were nonreactive or poorly reactive with mutants having the Ala-300→Asp change (Fig. 7A). In contrast, only MAb 16 lost reactivity with mutants K387A and K387A/T389A. The three site A-specific MAbs reacted with all mutants, although there were reductions in the reactivities of MAb 7 with A300D and MAb 6 with T389A and G299N.

A comparison of the HI and ELISA reactivities of MAbs 13, 15, 16, 8, and E with CPV-d, A300D, G299E, and K387A revealed similar patterns of reactivity, with one exception.

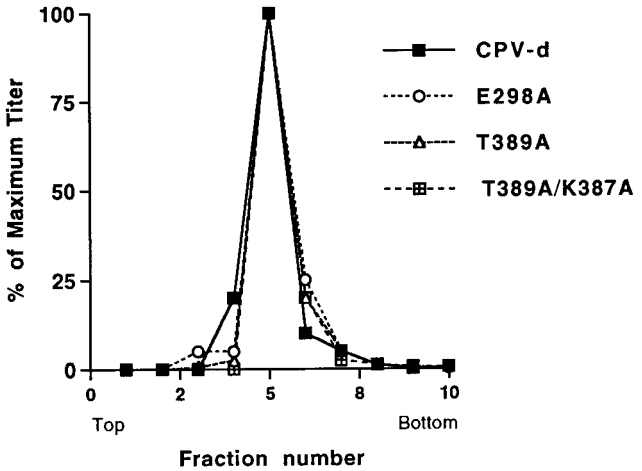

FIG. 3. Capsid formation from the expressed capsid proteins of the nonviable mutants. Cells were transfected with expression vector plasmids containing the VP1 and VP2 genes of nonviable mutants, and materials recovered from transfected cells were centrifuged in isopycnic CsCl gradients. The control was CPV-d empty capsids. HA titers in gradient fractions were determined, and the titers were plotted as a percentage of the titer in the peak fraction.

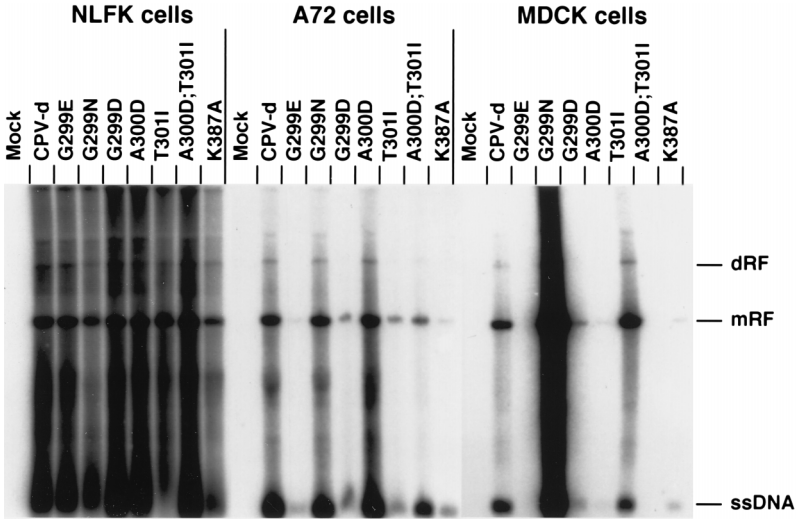

FIG. 4. DNA replication of CPV-d or mutant viruses in NLFK, A72, and MDCK cells. DNA was extracted from the cells 72 h (NLFK and A72 cells) or 48 h (MDCK cells) after virus inoculation, electrophoresed in 1% agarose gels, transferred to nylon membranes, and probed with ^{32}P-labeled viral DNA. The exposures of the blots were adjusted so that the intensities of the CPV-d DNAs were similar for each cell type. Single-stranded viral DNA (ssDNA) and mRF and dRF viral DNAs are indicated.

MAb 16, which did not react with G299E in the HI assay, bound well in the ELISA (Fig. 7B).

Capsid stability. A new salt bridge is present between Asp-300 and Arg-81 of a separate threefold axis-related monomer in the structure of mutant A300D (26); this new salt bridge may impart greater stability to the capsid. We examined mutants G299E, A300D, and K387A for changes in stability, as these mutants were restricted in their ability to infect certain canine cells and had either gained or lost a charged residue (Fig. 1 and 2). A comparison of the rate of heat inactivation of mutant and wild-type viruses indicated that mutants G299E and K387A and CPV-d all had similar 3- to 4-$\log_{10}$ reductions in titer after 40 min at 75°C (Fig. 8A). The susceptibility of the mutant and wild-type capsids to urea denaturation at pHs 7.5, 7.0, and 6.0 was examined. In control assays, both intact and denatured capsids were readily detected with a rabbit anticapsid serum. In contrast, a rabbit serum against SDS-denatured capsid proteins detected capsids denatured with 8 M urea but reacted to very low levels with untreated capsids (Fig. 8B). We used a mouse antipeptide serum against an epitope on the interior surface of the capsid to assess capsid disintegration. Mutant capsids G299E and A300D were less susceptible than CPV-d to urea denaturation, while K387A was similar to CPV-d (Fig. 8C). The three mutant and CPV-d capsids were all less susceptible to urea denaturation at pH 6.0 than at pH 7.5 or 7.0 (Fig. 8C).

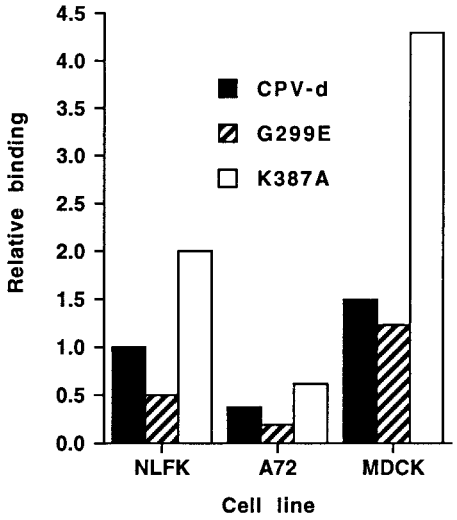

FIG. 5. Binding of [^{35}S]methionine-labeled CPV-d, G299E, or K387A capsids to NLFK, A72, or MDCK cells. The specific activities of the labeled viruses were estimated from the amounts of antigen detected by Western blotting, and the amounts of virus bound in each case are shown relative to the binding of CPV-d to NLFK cells.

DISCUSSION

In this study, we further characterized the biological functions associated with a region on the shoulder of the threefold spike of the CPV capsid which contains determinants of canine host range and a neutralizing antigenic site (site B) (37, 42, 50).

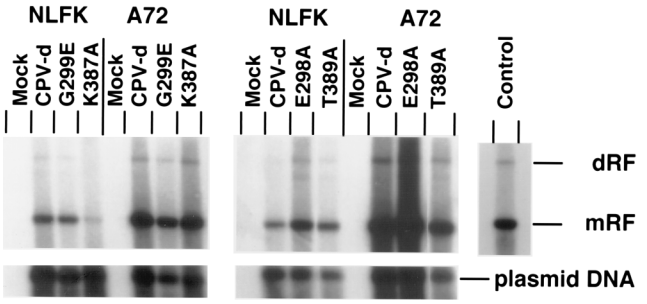

FIG. 6. (Top) Recovery of viral DNA 48 h after transfection of genome-length plasmids. Ten micrograms of plasmid DNA containing the CPV-d, G299E, E298A, K387A, or T389A genome was transfected into NLFK or A72 cells by use of Lipofectamine. Total DNA recovered 72 h later was digested for 3 h with *Dpn*I, electrophoresed in 1% agarose gels containing 1 μg of ethidium bromide per ml, and Southern blotted. mRF and dRF viral DNAs are indicated. (Bottom) DNA fragment generated by *Dpn*I from the viral sequence in the plasmid in the same gel, showing the relative amounts of plasmid DNA recovered from each of the transfected cell cultures.

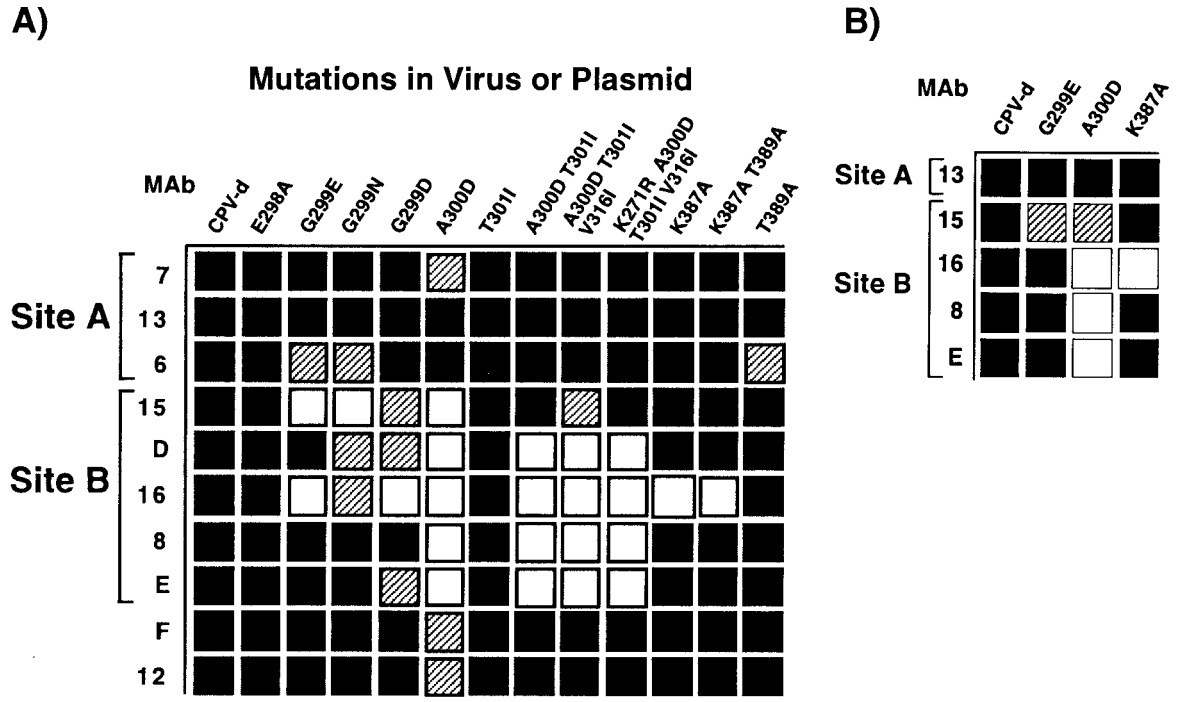

FIG. 7. Antigenic analysis of capsids prepared as infectious viruses or expressed as empty capsids from expression plasmids. (A) HI reactivity of a panel of MAbs with the mutant capsids shown relative to the reactivity of the MAbs with CPV-d. The reactivities of the MAbs are shown as filled squares if the HI titer was ≥10% that of CPV-d, hatched squares if it was <10% but >1% that of CPV-d, and open squares if it was <1% that of CPV-d. (B) ELISA results with CPV-d, A300D, G299E, and K387A and a subset of the MAbs shown in panel A. As shown previously (42), the filled squares indicate that the level of reaction was similar to that seen for CPV-d, hatched squares indicate <10% the level of reaction to CPV-d at a dilution at which the reaction with CPV-d is >90% saturating, and open squares indicate no reaction at any antibody dilution.

The results show that specific conformations of the shoulder region are necessary for CPV to retain the ability to infect canine cells. This conclusion is supported by our finding that changing residue 299, 300, or 301 on one polypeptide loop or residue 387 on a second interacting loop caused the virus to lose the ability to infect canine cells (Fig. 2 and 4). We examined two different canine cell lines. Although both cell lines were resistant to FPV and susceptible to CPV-d, they differed in susceptibility to different mutants. The three mutant viruses with Ala-300 replaced by Asp were able to infect A72 cells at lower detectable levels than CPV-d, but they were highly restricted in MDCK cells. In contrast, mutants with acidic residues replacing Gly-299 were markedly restricted in both canine cell lines (Fig. 1, 2, and 4). Acidic residues at position 299 have the potential to form salt bridges or other types of hydrogen bonds with Lys-387, Thr-389, or Arg-81. We speculate that the different gradations of host range restriction of A300D and G299E or G299D are due to differences in the structural constraints of their interchain bond formation (Fig. 2 and 4).

Infection of canine cells by the mutant viruses was blocked at an early stage, after cell binding but prior to viral genome replication. There was at most a fourfold difference in the binding of CPV-d and mutants G299E and K387A to canine or feline cells, whereas the difference in infectivity for canine cells was 3 to 5 $\log_{10}$-fold (Fig. 2 and 5). The host range restriction of the mutants in canine cells was not due to a defect in viral genome replication, as mutants G299E and K387A were both able to replicate normal levels of mRF and dRF DNAs after plasmid transfection into A72 cells (Fig. 6). Similarly, in other parvovirus models, host range restriction has been shown to occur prior to viral transcription but after cell surface binding (18, 23, 41).

We were unable to recover infectious virus following transfection of A72 or NLFK cells with plasmid clones of three mutants (E298A, T389A, and K387A/T389A). One reason for the nonviability could be that the capsids of these mutants did not assemble. However, when the capsid protein genes of these nonviable mutants were expressed from a mammalian expression plasmid, the proteins assembled into apparently normal empty capsids (Fig. 3). Other reasons for the nonviability of these mutants could be that their virions cannot infect canine or feline cells, the capsids may not package viral single-stranded DNA efficiently, or the mutations may interfere with replication of the DNA genome. Two nonviable mutants tested were able to replicate both mRF and dRF DNAs in NLFK and A72 cells transfected with their plasmid clones (Fig. 6). It is likely that the disruption of a hydrogen bond between the hydroxyl group of Thr-389 and the carbonyl group of Glu-298 (Fig. 1C) was responsible for the nonviable phenotype of the three nonviable mutants (E298A, T389A, and K387A/T389A). Residues Thr-389 and Lys-298 are very close to or bond with residues that were mutated in other, viable mutant viruses, suggesting that the structural changes which lead to nonviability also affect the same capsid functions which restrict host range in other mutants.

The original strain of CPV, which emerged in 1978, has been replaced worldwide by newer antigenic variants which have extended host ranges and infect cats as well as dogs (35, 45). These variants (termed CPV type 2a and type 2b) have changes of amino acid residues 300, 305, and 87 which are near or within the shoulder region (35), suggesting that these residue changes are responsible for the greater success of these CPV variants in dogs and for the gain of the in vivo feline host range (45). In addition, residues within this region are involved in

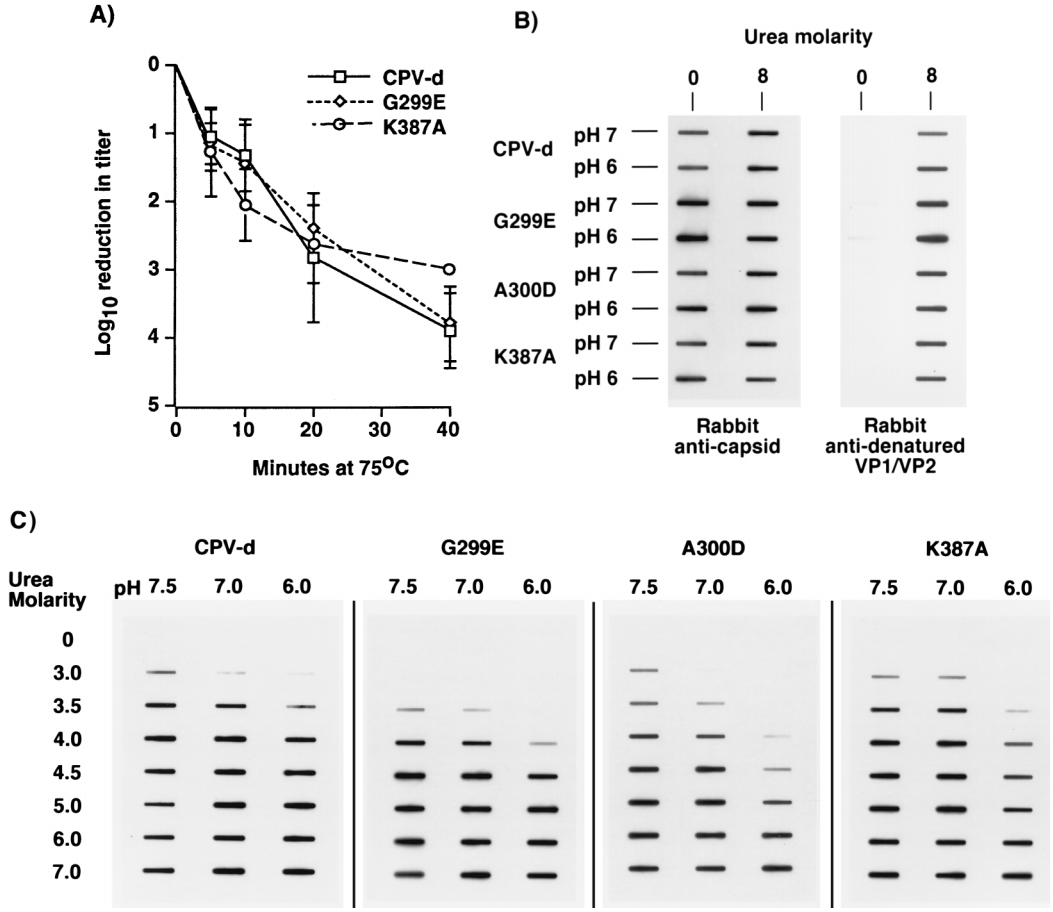

FIG. 8. Resistance of virus capsids to heat inactivation or urea denaturation. (A) Titers of CPV-d, G299E, and K387A after incubation for various times at 75°C. (B) CPV-d, G299E, A300D, and K387A full capsids at pH 7.0 or 6.0 were either untreated or incubated with 8.0 M urea and then bound to nitrocellulose membranes. Blots were probed with rabbit sera against either intact capsids or SDS-denatured VP1 and VP2, incubated with HRPO-conjugated goat anti-rabbit IgG followed by Supersignal, and exposed to X-ray film. (C) CPV-d, G299E, A300D, and K387A full capsids at pH 7.5, 7.0 or 6.0 in bis–Tris-HCl–NaCl buffer were either untreated or incubated with 3.0 to 7.0 M urea and then bound to nitrocellulose membranes. Blots were probed with mouse serum against a peptide containing the sequence of VP2 residues 258 to 270, incubated with HRPO-conjugated goat anti-mouse IgG followed by Supersignal, and exposed to X-ray film.

controlling the in vivo feline host range of FPV (44). Taken together, these findings emphasize that this region of the capsid is important for control of the natural host ranges and biological success of viruses in the feline parvovirus subgroup.

The antigenic differences between the mutant and CPV-d capsids are likely caused by small structural changes in antigenic site B; this site can be subdivided into a number of distinct epitopes (Fig. 7). It was of interest that MAb 16 bound to G299E capsids as avidly as it did to CPV-d capsids yet was unable to inhibit HA by G299E (Fig. 7). Sialic acids are the ligands responsible for HA by CPV, and they bind very close to the shoulder region (43). Therefore, a difference in the binding of sialic acid to G299E may explain the lack of HI reactivity of MAb 16.

Our results suggest that these host range determinants have very limited tolerance for conformational changes. A comparison of the structures of CPV-d and mutant A300D in the region of interest shows that Asp-300 forms a new salt bridge with Arg-81 on a threefold axis-related capsid monomer, accompanied by minor displacements (1.1 to 2.2 Å of the α-carbon) of residues 299, 300, and 301 (26). These relatively conservative structural changes of A300D led to a loss of its ability to infect canine MDCK cells.

The new salt bridge identified in the shoulder region of A300D was predicted to stabilize the capsid (26). Three other mutant viruses in this study (G299E, G299D, and K387A) have amino acid changes which may affect potential salt bridges between fivefold axis- or threefold axis-related VP2 monomers. We found that CPV-d, G299E, and K387A capsids were equally susceptible to heat inactivation (Fig. 8A). However, G299E and A300D capsids were clearly more resistant to urea denaturation than the CPV-d capsid (Fig. 8C). By analogy to A300D, it is likely that the glutamic acid at residue 299 of mutant G299E also interacts with Arg-81. In contrast, mutant K387A, which was predicted to lose a salt bridge with residue Glu-298, was similar to CPV-d in its susceptibility to urea denaturation. We do not know if the increased resistance of mutants G299E and A300D to urea denaturation has any functional relationship to their host range phenotype.

These results and those of previous studies (9, 22) show that host range determinants of CPV are situated in at least three regions of the capsid. In poliovirus, both surface and interior residues at a number of capsid locations have been shown to determine host range, and it has been suggested that these residues influence cell receptor binding or capsid conformational changes which occur upon receptor binding (12, 15, 27, 28). Thus, in poliovirus, host range can be determined by regions of the capsid which have different functions during the

infectious cycle of the virus (12, 14, 27). These capsid functions may be independent of one another but are more likely to be codependent, such that mutations affecting receptor binding can be compensated for by mutations affecting uncoating (11, 12).

How do these mutations control cell infection in a host-specific manner? Little is known about the process of cell infection by CPV. CPV capsids can bind to sialic acids as well as to several different cell proteins (4, 43). It has been hypothesized that the shoulder region may contain the footprint of the cell receptor for CPV (10). However, our results indicate that the mutations which we studied within this region do not affect primary receptor binding (Fig. 5). We cannot rule out the possibility that this region contains a binding site for a secondary receptor important for CPV infection of canine cells. In addition, CPV infection can be blocked by treating cells with NH_4Cl or chloroquine (5), suggesting that endosomal acidification has an effect on the CPV capsid that is necessary for successful virus entry. The capsids of picornaviruses, reoviruses, and adenoviruses undergo conformational changes during virus entry and infection (17, 20, 21, 24). The capsids of CPV-d and mutants G299E, A300D, and K387A were more resistant to urea denaturation at pH 6.0 than at pH 7.0 or 7.5 (Fig. 8C), suggesting that capsid conformational changes are associated with pH titration of charged residues (10). Whether these pH-dependent structural changes are important in infection remains to be determined.

In conclusion, we have identified a region of the capsid of CPV which is important for in vitro canine host range and virus viability. Infection of canine cells by CPV is a finely regulated process which requires very specific structures in several regions of the capsid. At present, we do not understand how these structures affect the virus-cell interactions involved in productive infection, but they all appear to affect one or more steps early in the infectious pathway, before the delivery of viral DNA to the cell nucleus.

ACKNOWLEDGMENTS

Wendy Weichert provided expert technical assistance. We thank Jean-Yves Sgro for providing assistance with Figure 1A.

This work was supported by grants AI28385 and AI33468 from the National Institutes of Health. J.S.L.P. is the recipient of a graduate research assistantship from the College of Veterinary Medicine, Cornell University.

REFERENCES

1. **Agbandje, M., C. R. Parrish, and M. G. Rossmann.** 1995. The structure of parvoviruses. Semin. Virol. **6:**299–309.
2. **Ball-Goodrich, L. J., R. D. Moir, and P. Tattersall.** 1991. Parvoviral target cell specificity: acquisition of fibrotropism by a mutant of the lymphotropic strain of minute virus of mice involves multiple amino acid substitutions within the capsid. Virology **184:**175–186.
3. **Ball-Goodrich, L. J., and P. Tattersall.** 1992. Two amino acid substitutions within the capsid are coordinately required for acquisition of fibrotropism by the lymphotropic strain of minute virus of mice. J. Virol. **66:**3415–3423.
4. **Barbis, D. P., S.-F. Chang, and C. R. Parrish.** 1992. Mutations adjacent to the dimple of the canine parvovirus capsid structure affect sialic acid binding. Virology **191:**301–308.
5. **Basak, S., and H. Turner.** 1992. Infectious entry pathway for canine parvovirus. Virology **186:**368–376.
6. **Bergeron, J., B. Hébert, and P. Tijssen.** 1996. Genome organization of the Kresse strain of porcine parvovirus: identification of the allotropic determinant and comparison with those of NADL-2 and field isolates. J. Virol. **70:**2508–2515.
7. **Binn, L. N., R. H. Marchwicki, and E. H. Stephenson.** 1980. Establishment of a canine cell line: derivation, characterization and viral spectrum. Am. J. Vet. Res. **41:**855–860.
8. **Bloom, M. E., B. D. Berry, W. Wei, S. Perryman, and J. B. Wolfinbarger.** 1993. Characterization of chimeric full-length molecular clones of Aleutian mink disease parvovirus (ADV): identification of a determinant governing replication of ADV in cell culture. J. Virol. **67:**5976–5988.
9. **Chang, S.-F., J.-Y. Sgro, and C. R. Parrish.** 1992. Multiple amino acids in the capsid structure of canine parvovirus coordinately determine the canine host range and specific antigenic and hemagglutination properties. J. Virol. **66:**6858–6867.
10. **Chapman, M. S., and M. G. Rossmann.** 1993. Structure, sequence, and function correlations among parvoviruses. Virology **194:**491–508.
11. **Colston, E., and V. R. Racaniello.** 1994. Soluble receptor-resistant poliovirus mutants identify surface and internal capsid residues that control interaction with the cell receptor. EMBO J. **13:**5855–5862.
12. **Colston, E. M., and V. R. Racaniello.** 1995. Poliovirus variants selected on mutant receptor-expressing cells identify capsid residues that expand receptor recognition. J. Virol. **69:**4823–4829.
13. **Cotmore, S. F., and P. Tattersall.** 1987. The autonomously replicating parvoviruses of vertebrates. Adv. Virus Res. **33:**91–174.
14. **Couderc, T., F. Delpeyroux, H. Le Blay, and B. Blondel.** 1996. Mouse adaptation determinants of poliovirus type 1 enhance viral uncoating. J. Virol. **70:**305–312.
15. **Couderc, T., J. Hogle, H. Le Blay, F. Horaud, and B. Blondel.** 1993. Molecular characterization of mouse-virulent poliovirus type 1 Mahoney mutants: involvement of residues of polypeptides VP1 and VP2 located on the inner surface of the capsid protein shell. J. Virol. **67:**3808–3817.
16. **Crandell, R. A., C. G. Fabricant, and W. A. Nelson-Rees.** 1973. Development, characterization and viral susceptibility of a feline (Felis catus) renal cell line (CRFK). In Vitro (Rockville) **9:**176–185.
17. **Fricks, C. E., and J. M. Hogle.** 1990. Cell-induced conformational change in poliovirus: externalization of the amino terminus of VP1 is responsible for liposome binding. J. Virol. **64:**1934–1945.
18. **Gardiner, E. M., and P. Tattersall.** 1988. Evidence that developmentally regulated control of gene expression by a parvoviral allotropic determinant is particle mediated. J. Virol. **62:**1713–1722.
19. **Gardiner, E. M., and P. Tattersall.** 1988. Mapping of the fibrotropic and lymphotropic host range determinants of the parvovirus minute virus of mice. J. Virol. **62:**2605–2613.
20. **Giranda, V. L., B. A. Heinz, M. A. Oliveira, I. Minor, K. H. Kim, P. R. Kolatkar, M. R. Rossmann, and R. R. Rueckert.** 1992. Acid-induced structural changes in human rhinovirus 14: possible role in uncoating. Proc. Natl. Acad. Sci. USA **89:**10213–10217.
21. **Greber, U. F., M. Willetts, P. Webster, and A. Helenius.** 1993. Stepwise dismantling of adenovirus 2 during entry into cells. Cell **75:**477–486.
22. **Horiuchi, M., H. Goto, N. Ishiguro, and M. Shinagawa.** 1994. Mapping of determinants of the host range for canine cells in the genome of canine parvovirus using canine parvovirus/mink enteritis virus chimeric viruses. J. Gen. Virol. **75:**1319–1328.
23. **Horiuchi, M., N. Ishiguro, H. Goto, and M. Shinagawa.** 1992. Characterization of the stage(s) in the virus replication cycle at which the host-cell specificity of the feline parvovirus subgroup is regulated in canine cells. Virology **189:**600–608.
24. **Kim, S., U. Boege, S. Krishnaswamy, I. Minor, T. J. Smith, M. Luo, D. G. Scraba, and M. G. Rossmann.** 1990. Conformational variability of a picornavirus capsid: pH-dependent structural changes of Mengo virus related to its host receptor attachment site and disassembly. Virology **175:**176–190.
25. **Kunkel, T. A.** 1985. Rapid and efficient site-specific mutagenesis without phenotypic selection. Proc. Natl. Acad. Sci. USA **82:**488–492.
26. **Llamas-Saiz, A. L., M. Agbandje-McKenna, J. S. L. Parker, A. T. M. Wahid, C. R. Parrish, and M. G. Rossmann.** 1996. Structural analysis of a mutation in canine parvovirus which controls antigenicity and host range. Virology **225:**65–71.
27. **Moss, E. G., and V. R. Racaniello.** 1991. Host range determinants located on the interior of the poliovirus capsid. EMBO J. **10:**1067–1074.
28. **Murray, M. G., J. Bradley, X.-F. Yang, E. Wimmer, E. G. Moss, and V. R. Racaniello.** 1988. Poliovirus host range is determined by a short amino acid sequence in neutralization antigenic site I. Science **241:**213–215.
29. **Nichols, G. E., J. C. Lovejoy, C. A. Borgman, J. M. Sanders, and W. W. Young, Jr.** 1986. Isolation and characterization of two types of MDCK epithelial cell clones based on glycosphingolipid pattern. Biochim. Biophys. Acta **887:**1–12.
30. **Paradiso, P. R., S. L. Rhode III, and I. I. Singer.** 1982. Canine parvovirus: a biochemical and ultrastructural characterization. J. Gen. Virol. **62:**113–125.
31. **Parker, J. S. L.** Unpublished data.
32. **Parrish, C. R.** 1994. The emergence and evolution of canine parvovirus—an example of recent host range mutation. Semin. Virol. **5:**121–132.
33. **Parrish, C. R.** 1990. Emergence, natural history, and variation of canine, mink, and feline parvoviruses. Adv. Virus Res. **38:**403–450.
34. **Parrish, C. R.** 1991. Mapping specific functions in the capsid structure of canine parvovirus and feline panleukopenia virus using infectious plasmid clones. Virology **183:**195–205.
35. **Parrish, C. R., C. F. Aquadro, M. L. Strassheim, J. F. Evermann, J.-Y. Sgro, and H. O. Mohammed.** 1991. Rapid antigenic-type replacement and DNA sequence evolution of canine parvovirus. J. Virol. **65:**6544–6552.
36. **Parrish, C. R., and L. E. Carmichael.** 1983. Antigenic structure and variation of canine parvovirus type-2, feline panleukopenia virus, and mink enteritis virus. Virology **129:**401–414.

37. **Parrish, C. R., and L. E. Carmichael.** 1986. Characterization and recombination mapping of an antigenic and host range mutation of canine parvovirus. Virology **148:**121–132.
38. **Parrish, C. R., P. H. O'Connell, J. F. Evermann, and L. E. Carmichael.** 1985. Natural variation of canine parvovirus. Science **230:**1046–1048.
39. **Reed, L. J., and H. Muench.** 1938. A simple method of estimating fifty per cent endpoints. Am. J. Hyg. **27:**493–497.
40. **Rossmann, M. G., and A. C. Palmenberg.** 1988. Conservation of the putative receptor attachment site in picornaviruses. Virology **164:**373–382.
41. **Spalholz, B. A., and P. Tattersall.** 1983. Interaction of minute virus of mice with differentiated cells: strain-dependent target cell specificity is mediated by intracellular factors. J. Virol. **46:**937–943.
42. **Strassheim, M. L., A. Gruenberg, P. Veijalainen, J.-Y. Sgro, and C. R. Parrish.** 1994. Two dominant neutralizing antigenic determinants of canine parvovirus are found on the threefold spike of the virus capsid. Virology **198:**175–184.
43. **Tresnan, D. B., L. Southard, W. Weichert, J.-Y. Sgro, and C. R. Parrish.** 1995. Analysis of the cell and erythrocyte binding activities of the dimple and canyon regions of the canine parvovirus capsid. Virology **211:**123–132.
44. **Truyen, U., M. Agbandje, and C. R. Parrish.** 1994. Characterization of the feline host range and a specific epitope of feline panleukopenia virus. Virology **200:**494–503.
45. **Truyen, U., J. F. Evermann, E. Vieler, and C. R. Parrish.** 1996. Evolution of canine parvovirus involved loss and gain of feline host range. Virology **215:**186–189.
46. **Truyen, U., and C. R. Parrish.** 1992. Canine and feline host ranges of canine parvovirus and feline panleukopenia virus: distinct host cell tropisms of each virus in vitro and in vivo. J. Virol. **66:**5399–5408.
47. **Tsao, J., M. S. Chapman, M. Agbandje, W. Keller, K. Smith, H. Wu, M. Luo, T. J. Smith, M. G. Rossmann, R. W. Compans, and C. R. Parrish.** 1991. The three-dimensional structure of canine parvovirus and its functional implications. Science **251:**1456–1464.
48. **Tullis, G. E., L. Labieniec-Pintel, K. E. Clemens, and D. Pintel.** 1988. Generation and characterization of a temperature-sensitive mutation in the NS-1 gene of the autonomous parvovirus minute virus of mice. J. Virol. **62:**2736–2744.
49. **Vasudevacharya, J., and R. W. Compans.** 1992. The NS and capsid genes determine the host range of porcine parvovirus. Virology **187:**515–524.
50. **Wikoff, W. R., G. Wang, C. R. Parrish, R. H. Cheng, M. L. Strassheim, T. S. Baker, and M. G. Rossmann.** 1994. The structure of a neutralized virus: canine parvovirus complexed with neutralizing antibody fragment. Structure **2:**595–607.